

1
2
3
4 **Phylogenomics of neglected flagellated protists supports a revised eukaryotic**
5 **tree of life**

6
7
8
9 Guifré Torruella^{1,2*}, Luis Javier Galindo^{1,3*}, David Moreira¹ and Purificación López-García¹

10
11 ¹ Ecologie Systématique Evolution, CNRS, Université Paris-Saclay, AgroParisTech, Gif-sur-
12 Yvette, France

13 ² Institut de Biología Evolutiva, UPF-CSIC, Barcelona, Catalonia, Spain.

14 ³ Department of Biology, University of Oxford, Oxford, United Kingdom.

15
16 * These authors equally contributed to this work.

17
18 For correspondence: guifftc@gmail.com, puri.lopez@universite-paris-saclay.fr

22 Eukaryotes radiated from their last common ancestor, diversifying into several supergroups
23 with unresolved deep evolutionary connections. Heterotrophic flagellates, often branching
24 deeply in phylogenetic trees, are arguably the most diverse eukaryotes. However, many of them
25 remain undersampled and/or *incertae sedis*. Here, we conducted comprehensive
26 phylogenomics analyses with an expanded taxon sampling of early-branching protists
27 including 22 newly sequenced transcriptomes (apusomonads, ancyromonads, *Meteora*). They
28 support the monophyly of Opimoda, one of the largest eukaryotic supergroups, with CRuMs
29 being sister to the Amorphea (amoebozoans, breviates, apusomonads, and opisthokonts –
30 including animals and fungi–), and the ancyromonads+malawimonads clade. By mapping traits
31 onto this phylogenetic framework, we infer a biflagellate opimodan ancestor with an excavate-
32 like feeding groove. Breviates and apusomonads retained the ancestral biflagellate state. Other
33 Amorphea lost one or both flagella, enabling the evolution of amoeboid shapes, novel feeding
34 modes, and palintomic cell division resulting in multinucleated cells, which likely facilitated
35 the subsequent evolution of fungal and metazoan multicellularity.

36

37

38 **Keywords:**

39 ancyromonad; apusomonad; free-living flagellate; *Meteora*; phylogenomics; transcriptomics;
40 RNAseq

41

42 Eukaryotes evolved from their prokaryotic ancestors in the early Proterozoic^{1,2} and rapidly
43 diversified into a multitude of lineages from an already complex last eukaryotic common
44 ancestor (LECA) that possessed all typical traits of extant eukaryotes³. The majority of
45 eukaryotes comprise hugely diverse unicellular, mostly flagellated and heterotrophic,
46 protists^{4,5}, although much of this diversity remains undescribed, as suggested by environmental
47 studies^{6,7}. Several eukaryotic lineages developed complex multicellularity, such as animals,
48 fungi, plants and brown algae, and/or acquired photosynthesis through the endosymbiosis of a
49 cyanobacterium or their algal derivatives^{4,5}. Heterotrophic protists are generally phagotrophic,
50 preying on bacteria or other protists⁴. Other heterotrophic eukaryotes such as fungi and
51 oomycetes became osmotrophic, feeding from the absorption of extracellularly digested
52 organic molecules; several of them evolved into parasites^{4,8}. With their diversity of trophic
53 modes, protists play crucial roles in ecosystem's networks and the carbon cycle⁹.

54 Eukaryotic lineages are currently known to form several large supergroups but their deep
55 phylogenetic relationships remain unresolved⁵, as is the root of the eukaryotic tree¹⁰. These
56 uncertainties can be explained by an inherent phylogenetic signal limitation due to a rapid
57 diversification in a short time span, methodological artefacts linked, among others, to
58 heterogeneous evolutionary rates, hidden paralogy and horizontal gene transfer, as well as to
59 patchy sampling across the eukaryotic diversity^{11,12}. Nonetheless, significant progress has been
60 achieved in recent years owing to the improvement of phylogenetic methods and to the
61 generation of genomic and/or transcriptomic data from poorly studied or newly identified
62 eukaryotes^{5,13}. The addition of this diversity has increasingly enlarged, reshaped and
63 consolidated eukaryotic supergroups. For instance, the long supported Opisthokonta clade,
64 comprising metazoans, fungi and their unicellular relatives (e.g. choanoflagellates,
65 ichthyosporeans, nucleariids, aphelids, rozellids)^{14,15} was found to form a robust supergroup,
66 the Amorphea, with classical amoeba (Amoebozoa) plus two groups of flagellated protists
67 previously considered *incertae sedis*, the amoeboflagellated Breviatea and the biflagellated
68 Apusomonadida¹⁶. Opisthokonta and Amoebozoa were previously thought to share a
69 uniflagellated ancestor¹⁷, and the root of the eukaryotic tree to lie between this Unikonta clade
70 and the rest of eukaryotes (Bikonta)¹⁸. The latter clustered several lineages sharing a
71 biflagellate ancestor, including Archaeplastida (glaucophytes, red algae, green algae and
72 plants) and SAR, composed of Stramenopiles (e.g. oomycetes, diatoms, brown algae),
73 Alveolata (e.g. dinoflagellates, ciliates) and Rhizaria (e.g. radiolarians, cercozoans)¹⁸.
74 However, the nested position of apusomonads (represented at the time by the genome of a
75 single species) within unikonts rejected the idea of a uniflagellated ancestor, and the new names
76 Opimoda and Diphoda were proposed for those redefined major splits¹⁹. Archaeplastida and
77 SAR, together with other lineages of unicellular protists, many photosynthetic (cryptophytes,
78 haptophytes), and their allies (e.g. telonemids, centrohelids, *Palpitomonas*) often cluster in a
79 large supergroup called Diaphoretickes^{20,21}. At the same time, another group of poorly known
80 protists called CRuMs (collodictyonids, rigifilids, and *Mantamonas*) appears to branch as sister
81 to the Amorphea^{5,22}. To complete the global picture, Excavata, once thought to be a major
82 eukaryotic supergroup characterized by the shared phenotypic feature of a ventral feeding
83 groove, lacks molecular phylogenetic support and is no longer considered monophyletic, being
84 split into Discoba (e.g. euglenids, jakobids), Malawimonadida²⁰ and Metamonada (e.g.
85 trichomonads, *Trimastix*, *Carpediomonas*)^{5,19}.

86 If the inclusion of phylogenomic data for many newly described flagellates has confirmed
87 some eukaryotic supergroups, many lineages of heterotrophic flagellates are yet to find a home
88 in the eukaryotic tree and remain *incertae sedis*. This is the case of ancyromonads²³ or
89 malawimonads²⁰, so far not clearly related to any eukaryotic supergroup. Other newly
90 described phylum-level lineages such as *Provora*²⁴ (including *Ancoracysta*²⁵)
91 *Hemimastigophora*²¹ and *Meteora*^{26,27} also branch deeply in the eukaryotic tree, although
92 showing some affinity with the Diaphoretickes. In general, many of these difficult-to-place
93 lineages are represented by one or few representative species available in culture. However,
94 they are most likely undersampled and encompass a wider within-group diversity. This can be
95 illustrated by apusomonads²⁸, for which the use of specific 18S rRNA gene primers revealed a
96 broad diversity of these gliding flagellates in freshwater and marine benthos across the globe²⁹.
97 Getting these tiny predators in culture for further study is challenging for several reasons. They
98 depend on specific bacterial or eukaryotic prey which, in turn, are not necessarily easy to
99 identify and maintain. Also, being higher in the trophic chain, they are in lower abundances in
100 their native ecosystems and, hence, underrepresented in metagenomic data. Likewise,
101 metagenomic studies rarely target sediment samples, where many of these organisms roam.
102 Sediment-dwelling heterotrophic flagellates therefore remain largely understudied despite their
103 long appreciated ecological role as grazers³⁰, and their incorporation to global phylogenetic
104 analyses can help resolving the eukaryotic tree^{21,24,27}. Here, we generated almost complete
105 transcriptomes of diverse members of the Apusomonadida (14 species) and Ancyromonadida
106 (7 species) that we recently cultured from different marine and freshwater environments^{31,32},
107 as well as the type species of *Meteora sporadica*, which we cultured from Mediterranean
108 samples²⁶. Our phylogenomic analyses with an expanded dataset of early-branching
109 heterotrophic flagellates resolve the internal evolutionary relationships within Apusomonadida
110 and Ancyromonadida and shed new light onto the eukaryotic tree, reinforcing the Opimoda
111 monophyly. The distribution of complex phenotypic traits in this phylogenomic framework,
112 notably the presence and number of flagella, the occurrence of pseudopodia or the
113 karyokinesis-cytokinesis coupling, helps inferring ancestral states and crucial steps that
114 conditioned lifestyles and subsequent major evolutionary trends along the natural history of
115 eukaryotes.

116

117

118 **Results and Discussion**

119

120 **High-quality curated transcriptomes for phylogenomic analysis**

121 We considerably enriched the number of available transcriptomic datasets for members of the
122 Apusomonadida²⁸ Karpov & Mylnikov 1989, and Ancyromonadida²³ Atkins et al. 2000 by
123 sequencing polyA-containing transcripts of recently cultured species spanning the diversity of
124 these two clades^{31,32}. We also generated transcriptome data for the Mediterranean type strain
125 of *Meteora sporadica*²⁶ (Supplementary Table 1). Since these eukaryotic species were in co-
126 culture with diverse bacteria and sometimes other protists, we established a pipeline
127 (Supplementary Fig.1) to eliminate contaminant sequences and retained only targeted protein-
128 coding genes for subsequent phylogenomic analyses (see Methods). After the strict manual

129 curation of these datasets, we obtained a set of highly complete transcriptomes, as assessed by
130 the presence of universal single-copy genes using BUSCO³³. Most of our transcriptomes were
131 more than 80% and up to ~93% complete (Supplementary Table 1). Regarding the presence of
132 the selected 303 phylogenetic markers for phylogenomic analyses (Methods), they contained
133 relatively few missing markers (~6% and 8%, on average, for apusomonads and acyromonads,
134 respectively; 8.5% for *Meteora*) and total amino acid gaps in the final multimarker alignment
135 (7.9% and 11.7% , on average, for apusomonads and acyromonads, respectively; 11.5% for
136 *Meteora*). These represented comparable or even more complete datasets than those for the few
137 previously 454-sequenced transcriptomes for the same clades³⁴, as well as the only available
138 apusomonad genome, that of *Thecamonas trahens*³⁵ (13% missing data), and the
139 transcriptomes of the apusomonad *Striomonas* (formerly *Nutomonas*) *longa*³⁶ (15.9% gaps)
140 and the acyromonads²² *Acyromonas kenti* (42.83% gaps) and *Fabomonas tropica* (24.2%
141 gaps) (Supplementary Table 2).

142 The less complete transcriptomes in our newly generated datasets were those of
143 *Apusomonas proboscidea* and *Nutomonas limna terrestis* (29.2% and 24.4% gaps,
144 respectively). *A. proboscidea* was co-cultured with a stramenopile contaminant. In general, the
145 less complete transcriptomes corresponded to those that suffered most cross-contamination;
146 other examples were the acyromonad *Nyramonas silfraensis* (14.9% gaps) and the
147 apusomonad *Chelonemonas dolani* (14.52% gaps) (Supplementary Table 2). Although we
148 could easily remove cross-contaminant sequences when analysing single marker trees, we were
149 very strict not to include any potential contamination from prey or co-cultured microorganisms
150 in order to retain only high-quality data (see Methods; Supplementary Fig.1. and
151 Supplementary Tables 3-4). In addition, since de novo transcriptomes are prone to show
152 artificially duplicated sequences in comparative genomics analyses, we tested the inferred
153 oligopeptide redundancy by clustering sequences with CD-HIT at 90% identity. This procedure
154 removed few such oligopeptide sequences for most species (6.5% on average), except for the
155 highly duplicated *Mylnikovia oxoniensis* (~42%), as well as for *Multimonas media* (20.5%),
156 *Apusomonas australiensis* (15.5%) and *Cavaliersmithia chaoae* (9.6%). However, the removal
157 of this redundancy did not affect the BUSCO completeness (Supplementary Table 3) and the
158 information available for the set of conserved proteins used in phylogenomic analyses.

159

160 **Phylogenomic analyses of an expanded dataset of heterotrophic flagellates**

161 To infer the evolutionary relationships among major eukaryotic supergroups, we included data
162 from our transcriptomes and from a large representation of heterotrophic flagellates. Our final,
163 manually curated dataset contained 303 concatenated markers, corresponding to 97,171 amino
164 acid positions, for a total of 101 selected taxa (Supplementary Table 2). We applied state-of-
165 the-art complex mixture models of sequence evolution in both maximum likelihood (ML) and
166 Bayesian inference (BI) methods to alleviate putative homoplasy and long-branch attraction
167 artefacts. The ML tree was reconstructed using the PMSF approximation of the model
168 LG+C60+F+G (Supplementary Fig.2), and the BI trees, with the CAT-GTR (Supplementary
169 Fig.3) and CAT-Poisson (Supplementary Fig.4) models of sequence evolution, respectively.
170 BI and ML phylogenomic analyses yielded congruent tree topologies for major eukaryotic
171 groups, with only minor changes in the position of some branches (Fig.1 and Supplementary
172 Figs.1-3).

173 All our analyses retrieved the monophyly of Apusomonadida and Ancyromonadida with
174 maximal support. The internal relationships within each of these groups were overall stable,
175 except for very minor uncertainties (Fig.1). The Apusomonadida comprised two major clades,
176 A and B, both grouping a mix of marine and freshwater species showing an overall internal
177 topology congruent with that based on 18S rRNA gene phylogenies³¹. Clade A grouped species
178 characterized by an elongated *Amastigomonas*-type morphology and relative large cell size (~8
179 µm; genera *Multimonas*, *Podomonas*, *Cavaliersmithia*, *Mylnikovia* and *Catacumbia*). Clade B
180 comprised the Thecamonadinae, also grouping species with the elongated *Amastigomonas*-type
181 morphology but of smaller size (~5 µm cell diameter; genera *Singekia*, *Karpovia*,
182 *Chelonemonas* and *Thecamonas*)³¹, and the Apusomonadinae, which grouped the genera
183 *Apusomonas*, characterized by rounded cells, and *Manchomonas*, exhibiting elongated and
184 larger cells (9.5 µm)³⁷. The only internal uncertainty within the apusomonads concerned the
185 placement of *Manchomonas*, which branched sister to the Thecamonadinae, instead of
186 *Apusomonas*, in BI trees using the CAT-GTR model, albeit with modest support (0.74 posterior
187 probability –PP–; Supplementary Fig.3). These topological differences may be a consequence
188 of the high percentage of missing data from *Manchomonas bermudensis* (only 62 out of the
189 303 selected markers proteins, 90.49% gaps), with only EST data available for this species (F.
190 Lang, unpublished; Supplementary Table 2). Apusomonadida formed a fully supported clade
191 with Opisthokonta, which was sister to the Breviatea (Obazoa). In turn, this Obazoa clade was
192 sister to Amoebozoa with full support (Amorphea clade) and, the Amorphea to the CRuMs
193 with very good to full support, forming the supergroup Podiata³⁸ (Fig.1).

194 Similarly, we retrieved the monophyly of the two described ancyromonad families,
195 Ancyromonadidae and Planomonadidae³⁹, and the recovered internal topology for the clade
196 was again congruent with that based on 18S rRNA genes³². Within Ancyromonadidae, we
197 retrieved a clade of marine representatives (*Caraotamonas* and *Ancyromonas* species) and
198 another of freshwater members (*Striomonas*, *Nutomonas* and *Nyramonas*) (Fig.1). However,
199 we only retrieved the monophyly of Planomonadidae, including *Planomonas* and *Fabomonas*,
200 with ML; BI analyses placed *Fabomonas* as the earliest-branching ancyromonad, sister to all
201 other ancyromonad genera (0.8 PP for CAT-GTR, and 0.99 PP for CAT-Poisson;
202 Supplementary Figs.3-4). Interestingly, malawimonads²⁰, traditionally classified within
203 Excavata⁴⁰⁻⁴², branched sister to the ancyromonads in our ML tree (Fig.1, Supplementary
204 Fig.2), in line with some previous analyses^{22,34}. Ancyromonadida and Malawimonadida formed
205 a monophyletic supergroup with Amorphea and CRuMs, the Opimoda, fully supported in the
206 ML tree and well supported in BI with CAT-GTR (0.99 PP). However, in the BI analyses,
207 Ancyromonadida appeared as the earliest-branching lineage within Opimoda (0.99 PP and 0.75
208 PP under CAT-GTR and CAT-Poisson models, respectively), Malawimonadida being sister to
209 the Podiata clade (0.98 PP and 0.73 PP under CAT-GTR and CAT-Poisson models
210 respectively) (Fig.1; Supplementary Figs.2-4).

211 To test whether the aforementioned uncertainties in our phylogenomic tree, i.e. the position
212 of *Manchomonas* within Apusomonadida, that of *Fabomonas* within Ancyromonadida and the
213 position of Malawimonadida, could result from marked differences in evolutionary rate, we
214 analysed the stability of the respective branches in the tree against alternative topologies
215 (Fig.2a-c) after progressive removal of the fastest-evolving sites in the alignment (5% at a
216 time). As can be seen in Fig.2d, the monophyly of *Manchomonas* and *Apusomonas* was

217 strongly supported until only 15% of the data remained. Likewise, the monophyly of
218 *Planomonas* and *Fabomonas* was fully supported until less than 25% of sites remained. In the
219 case of malawimonads, we monitored the statistical support for, in addition to the two observed
220 topologies in our analyses, the monophyly of malawimonads and Discoba. We followed, as
221 control, the monophyly of Opisthokonta, which were fully supported until 15% of sites
222 remained (Fig.2d). We recovered general low support for the two observed alternatives, albeit
223 the statistical support for the monophyly of malawimonads and ancyromonads was always
224 much higher than malawimonads as sister of the Podiata. By contrast, the monophyly of
225 malawimonads and Discoba was never observed (Fig. 2d).

226 Although our eukaryotic tree was not rooted with an external outgroup, we included the
227 widest possible diversity of free-living protists also on the Diphoda¹⁹ side, including
228 heterotrophic flagellates when possible. We arbitrarily rooted our trees using the excavate clade
229 Metamonada, with the inclusion of the relatively short-branching *Trimastix* species (Fig.1). As
230 expected, Metamonada appeared paraphyletic with respect to Discoba^{43,44}. Also, we recovered
231 the monophyly of Diaphoretickes with full support (Fig.1). Within Diaphoretickes, the SAR
232 supergroup also received full support. However, the monophyly of SAR and telonemids found
233 in some analyses (the TSAR group⁴⁵) was not observed. Telonemids branched within or sister
234 to Haptista, albeit with moderate-to-low support (Fig.1). The Archaeplastida clade was
235 recovered with moderate (96%; ML) to full support (1 PP; BI CAT-GTR) and included the
236 Picozoa as sister to Rhodelphida + Rhodophyta, in agreement with recent observations⁴⁶, albeit
237 with full support only from BI analyses using CAT-GTR. We also recovered with full support
238 the widely accepted monophyly of Archaeplastida and Cryptista^{21,46}. Finally, we retrieved the
239 monophyly of *Ancoracysta* (Provora)²⁵, Hemimastigophora²¹ and the *Meteora sporadica* type
240 strain CRO19MET²⁶ with full ML support, as has been recently observed with another strain
241 of *M. sporadica*²⁷. *Ancoracysta* and other Provora members have also been suggested to form
242 a monophyletic group with Hemimastigophora²⁴. Our results thus provide additional support
243 for this new supergroup of morphologically diverse predatory protists.

244

245 **Evolution of major phenotypic traits during the early eukaryotic radiation**

246 Our results suggest that, although resolving the phylogenetic tree of eukaryotes is challenging,
247 the topology of the tree can be stabilized with the incorporation of a more balanced taxon
248 sampling, including a wider representation of deep-branching free-living protists, combined
249 with the use of appropriate phylogenetic reconstruction approaches. Our phylogenomic
250 analyses including an expanded sampling of apusomonads and ancyromonads converge to a
251 rather stable topology for some major clades, notably in the Opimoda supergroup and its
252 increasingly nested phylogenetic clades (Podiata, Amorphea, Obazoa), which appear sister to
253 a clade containing the ancyromonads and, most likely, the malawimonads (Fig.1). This
254 phylogenetic framework allows to comparatively assess the distribution of complex phenotypic
255 features, infer the ancestral states for the different clades and propose plausible evolutionary
256 scenarios for trait evolution. Obviously, the availability of morphological and structural data is
257 still limited, many morphological features may not be homologous, and more biodiversity
258 alongside ultrastructural and phylogenetic analyses with, notably, the inference of a rooted tree
259 of eukaryotes (e.g. using mitochondrial or Asgard archaeal-derived markers) will be needed to
260 validate and/or complete this emerging evolutionary scheme (Fig.3).

261 It is interesting to note that some large clades, notably the ancyromonads, show apparent
262 phenotypic stasis. Indeed, ancyromonads have comparable levels of sequence divergence to
263 those of other morphologically and structurally diverse lineages such as Amoebozoa or
264 Opisthokonta, but have retained a constrained morphotype for hundreds of million years,
265 suggesting an efficient adaptation to their predatory lifestyle in benthic and soil ecosystems.
266 Unlike apusomonads, there seems to be no obvious morphological differences between
267 ancyromonad family members in terms of cell size, shape or any other particular feature
268 observable under light microscopy³². Ecologically, ancyromonads include marine and
269 freshwater species, with the topology of the tree for the current taxon sampling suggesting a
270 single transition from marine ancestors to a clade of freshwater genera (*Nyramonas*,
271 *Nutomonas*, *Striomonas*; Fig.1). Accordingly, the last common ancestor of ancyromonads was
272 likely marine and resembled extant species, having bean-shaped flattened biflagellate cells with
273 a short anterior flagellum and a rostrum with extrusomes³². Although ancyromonads have a
274 dorsal pellicle, a complex cytoskeleton and a ventral groove for feeding, they do not bear the
275 bona fide excavate groove or actin-based pseudopods similar to those of diverse Obazoa³²
276 (Fig.3). By contrast, apusomonads, another diverse clade with high internal evolutionary
277 divergence, exhibit some apparent morphological differences and ecological variation, with
278 marine-freshwater transitions having occurred multiple times during their evolution^{29,31}
279 (Fig.1). Within clade A, members of the four described genera exhibit a short proboscis sleeve
280 as compared to the cell body length, as well as more-prominent pseudopodia than other
281 apusomonads³¹. Additionally, *Podomonas* has a tusk, a character also present in
282 Thecamonadinae⁴⁷. *Multimonas* also displays a potential tusk, posterior extrusomes⁴⁸ and
283 division by binary and multiple fission. *Podomonas* and *Mylnikovia* possess refractile granules
284 running in parallel to the posterior flagellum⁴⁹. All these characteristics can be found in other
285 apusomonads³¹. In clade B, if *Karpovia* or *Singekia* present a tusk, not clearly observed yet
286 under optical microscopy, they would also fit the description of the subfamily
287 Thecamonadinae⁴⁷, alongside trailing pseudopodia³¹. Also within clade B, *Manchomonas* and
288 *Apusomonas* share some morphological similarities, such as few pseudopods, a hidden
289 posterior flagellum, the absence of tusks, and some ultrastructural features⁵⁰. *Manchomonas*
290 has the largest observed sleeve compared to other apusomonads of elongated shapes, while
291 *Apusomonas* exhibits a unique structure called mastigophore. Given the widespread elongated,
292 *Amastigomonas*-type, cell shape in apusomonads, this seems the ancestral phenotype for the
293 group, with the rounded *Apusomonas* cells being derived. Although there is considerable
294 morphological variation within the group and many environmental species remain to be
295 described²⁹, the available information suggests that the last apusomonad common ancestor had
296 a typical elongated cell type, with dorsal pellicle, ventral feeding groove, actin-based
297 pseudopodia, and proboscis (likely with a short sleeve), probably with a tusk and able to divide
298 by multiple fission (Fig.3).

299 In our phylogenomic tree, malawimonads and ancyromonads were sister groups (Fig.1). If
300 confirmed, this would imply that this clade is one of the earliest branching lineages after the
301 Opimoda-Diphoda split. Alternatively, malawimonads could be sister to the Podiata. Whatever
302 the actual topology, since both clades encompass small bacterivorous heterotrophic
303 biflagellates with a, likely homologous⁵¹, ventral feeding groove^{20,32,52}, the last common
304 ancestor of Opimoda most likely shared this excavate-like phenotype (Fig.3). Furthermore,

305 since excavates are likely paraphyletic^{22,24,35}, with Metamonada and Discoba branching deeply
306 in the eukaryotic tree (Fig.1), it might be argued that the ancestral LECA phenotype also
307 corresponded to that of an excavate-like biflagellate⁵³, irrespective of the specific position of
308 the root¹⁰ (Fig.3). This seems further supported by the strong conservation of the microtubular
309 cytoskeleton and the flagellar apparatus⁵⁴ across eukaryotes⁵⁵. From such an ancestor,
310 acyromonads developed a dorsal pellicle and a rostrum with extrusomes, losing the flagellar
311 vanes and shortening the anterior flagellum²⁰. It is possible that the opimodan ancestor was a
312 marine planktonic biflagellate that lost free swimming capabilities and adapted to glide on
313 benthic substrates. Without the excavate physical constraints for feeding that are intertwined
314 with the flagellar motility⁵¹, the acyromonad morphotype might have easily evolved (Fig. 3).
315 Bearing a dorsal pellicle, acyromonads maintained ventral feeding, keeping the posterior
316 flagellum attached to the surface, which is likely at the origin of the “twitch- yanking”
317 movement for feeding³².

318 Our phylogenomic tree supported the monophyly of Amorphea (Amoebozoa, Breviatea,
319 Apusomonadida and Opisthokonta) and CRuMs (Fig.1). This clade had already been proposed
320 to occur based on the shared capability to produce pseudopodia across their members and,
321 accordingly, named Podiata³⁸. The last common ancestor of Amorphea was clearly able to
322 produce pseudopodia (Fig.3). However, the available cell biology descriptions for CRuMs are
323 still limited²² and the presence of some features, such as a pellicle homologous to that of
324 apusomonads and acyromonads⁵⁶, is unclear. Likewise, the presence of true pseudopodia in
325 some species (e.g., *Micronuclearia* and *Rigifila*) needs further confirmation. Nonetheless, at
326 least some *Mantamonas* species (e.g. *M. plastica*) do bear pseudopodia⁵⁷ and, accordingly, the
327 ancestor of the group. Mantamonadida have a stable phylogenetic position⁵⁸ and might have
328 retained some of the ancestral features of CRuMs; indeed, *Mantamonas* share some similarities
329 with acyromonads, notably the possession of small flattened cells with a short anterior
330 flagellum and benthic/soil-associated lifestyles. However, the other CRuM lineages
331 (Diphylloida and Hilomonadea) include larger, freshwater planktonic species, also possessing
332 a ventral groove^{56,59}. Populating the CRuMs’ branch with new described members should help
333 to ascertain trait evolution within this clade.

334 The Amorphea contain the most diversified and studied lineages of the opimodan side of
335 the eukaryotic tree, Amoebozoa and Opisthokonta. These clades exhibit more diverse and
336 derived morphoplans than the two other amorphean lineages, Apusomonadida and Breviatea.
337 Amoebozoa and Opisthokonta lost one or both flagella^{60,61}. Biflagellate protists have complex
338 microtubular cytoskeletons that impose severe structural constraints on their cell shape, such
339 that flagellar loss, freeing those constraints, likely facilitated the evolution of more diverse
340 morphoplans. This increased morphological evolvability linked to concomitant changes in
341 selective pressures allowed the exploration of novel cell shapes (e.g. amoeboid), feeding modes
342 (e.g., osmotrophy) and cell-cell interactions (e.g., multicellularity), as currently observed
343 across this clades³⁴. By contrast, both Breviatea and Apusomonadida, being paraphyletic within
344 the Obazoa, can be inferred to have retained the ancestral biflagellate state alongside other
345 features likely present in the obazoan ancestor (Fig.3). Both lineages encompass small
346 bacterivorous amoeboflagellates that phagocytize prey using pseudopodia (unlike
347 acyromonads or excavates)⁴⁹. Breviates are anaerobic and possess gliding and swimming
348 forms, lack a pellicle and display more pronounced amoeboid shapes than apusomonads¹⁶.

349 Apusomonads comprise gliding, elongated, semi-rigid amoeboflagellates with an anterior
350 proboscis and a dorsal pellicle allowing ventral feeding similarly to ancyromonads^{31,47}.
351 Interestingly, both breviates and apusomonads can divide palintomically, i.e. their karyokinesis
352 is uncoupled from cellular division leading, at least transiently, to multinucleated cells. The
353 ability to generate multinucleated cells is also widespread across amoebozoans and
354 opisthokonts, including several unicellular relatives of animals (e.g. corallochytrids)⁶² and
355 fungi (e.g. aphelids)¹⁴. It seems increasingly clear that the occurrence of cenocytic (i.e.,
356 multinucleated) stages was important along the road to metazoan multicellularity¹⁵. Therefore,
357 the ancestral Amorphea capability to produce multinucleated cells appears intriguingly crucial
358 for the subsequent evolution of plasmodial growth, and metazoan and hyphal-based fungal
359 multicellularity.

360

361

362 **Methods**

363

364 **Protist culture, RNA extraction and transcriptome sequencing**

365 The 22 species of heterotrophic flagellate protists from which we generated transcriptome data
366 were previously isolated or enriched from benthos of marine or freshwater ecosystems or soil,
367 and included apusomonads³¹, ancyromonads³² and the type strain of *Meteora sporadica*²⁶
368 (Supplementary Table 1). Soil and freshwater flagellates were grown in Volvic water with 1%
369 yeast tryptone (YT), and marine flagellates in 0.2 micron-filtered seawater with 1% YT
370 medium or Cerophyl medium. Flagellates were grown in flat cell culture flasks with ~10 ml of
371 medium, just to cover the bottom surface (75 cm²). The gliding protist cells from high-density
372 cultures were collected by gently scratching the bottom of the flask with a cell scraper and
373 pooled in 50 ml Falcon tubes. Cells were pelleted by centrifugation at 10°C for 15 minutes at
374 15,000g. Total RNA for each species was extracted with the RNeasy mini Kit (Qiagen)
375 following the manufacturer protocol, including DNase treatment. Purified RNA was
376 quantified using a Qubit fluorometer (ThermoFisher Scientific). For each species, cDNA
377 Illumina libraries were constructed after polyA mRNA selection, tagged and paired-end (2 ×
378 150 bp) sequenced with Illumina NovaSeq 6000 S2 (Eurofins Genomics, Germany) in three
379 different sequencing runs (NG-22350, NG-24277, NG-25209; Supplementary Fig.1 and
380 Supplementary Table 4). Sequence statistics and accession numbers are provided in
381 Supplementary Table 1.

382

383 **Transcriptome assembly and decontamination**

384 The quality of Illumina sequences was checked with FastQC⁶³ v0.11.8. High-quality reads were
385 retained and used for transcriptome *de novo* assembly using Spades⁶⁴ v3.13.1 66 with -rna
386 mode and default parameters. Cross-contamination of transcripts among multiplexed cDNA
387 libraries within the same sequencing run were detected and removed using CroCo⁶⁵ v1.2
388 (Supplementary Fig.1, Supplementary Tables 3-4). We translated the remaining transcripts into
389 oligopeptides using TransDecoder v5.5 (<https://github.com/TransDecoder/>) with the script
390 LongOrfs and clustered them with CD-HIT⁶⁶ v4.8.1 at 100% identity. Predicted oligopeptides
391 of non-eukaryotic origin were removed using similarity search against a custom protein

392 database (BAUVdb: bacteria, archaea, eUkaryotes and viruses). BAUVdb included 32
393 reference genomes of eukaryotic species spanning all supergroups (Supplementary Table 5) as
394 well as, respectively, 62,291 and 3,412 bacterial and archaeal genomes from the Genome
395 Taxonomy DataBase, GTDB⁶⁷ release 207, 361,930 viral genomes from the reference viral
396 database (RVDB)⁶⁸ and RVDB proteins⁶⁹ clustered using CD-HIT at 90% identity and
397 coverage. To discriminate target eukaryotic sequences from those of alien origin, we then
398 applied Diamond⁷⁰ v2.0.14.152 in ultra-sensitive mode setting an e-value threshold of 1e-3 for
399 a maximum of 100 hits. From the tabular output, eukaryotic oligopeptides were retained if
400 *Thecamonas trahens* or five eukaryotes were the first hits. Eukaryotic oligopeptides were
401 automatically annotated using eggNOG-mapper⁷¹ using all orthologs and all annotations as
402 evidence. The number of identified single-copy markers from BUSCO³³ v5.2.2 were used as a
403 proxy for gene set completeness using the eukaryote database db10. All transcripts and
404 oligopeptides generated in this study are available in the figshare repository
405 (10.6084/m9.figshare.22148027). Since *A. proboscidea* MPSANABRIA15 was co-cultured
406 with a difficult-to-eliminate stramenopile contaminant (belonging to the genus
407 *Paraphysomonas*, as inferred from its 18S rRNA gene sharing ~98% pairwise identity with
408 members of this genus), we also sequenced the transcriptome of the latter from a
409 monoeukaryotic culture (NCBI biosample SRR23610779). To decontaminate the apusomonad
410 set of proteins from stramenopile sequences, eukaryotic proteins of *A. proboscidea*
411 MPSANABRIA15 were used as queries in BLASTP (minimum e-value of 1e-25) against a
412 protein database with the closest related taxa (PROMEX), our own stramenopile contaminant,
413 plus three publicly available *Paraphysomonas* transcriptomes: MMETSP1103, MMETSP0103
414 and MMETSP1107. Eukaryotic oligopeptides were considered contaminant when they had
415 only stramenopile hits or, in the case of hits in both lineages, when the pairwise identity,
416 weighted by coverage, was higher in stramenopiles than in PROMEX.
417

418 Phylogenomic analyses

419 Our phylogenomic dataset was updated from a previous paneukaryotic study with 104 taxa and
420 351 conserved markers²¹. To that dataset, we added the corresponding identified markers from
421 recently sequenced genomes/transcriptomes of early-branching eukaryotes^{45,72-75} and from our
422 22 flagellate brut transcriptomes (Supplementary Table 2). To identify the selected
423 phylogenetic markers in these transcriptomes, we queried these datasets with the 351 marker
424 sequences from *Homo*, *Saprolegnia*, *Spizellomyces* and *Diphylleia* with BLASTp and retrieved
425 all possible homologs. Each marker from the 230 taxa representing all eukaryotic supergroups,
426 was aligned with MAFFT⁷⁶ v7.427 77 (L-INS-i with 1000 iterations), and trimmed using
427 Trimal⁷⁷ v1.4.rev22 in automated mode. Approximate-maximum likelihood single marker trees
428 were inferred from each trimmed alignment using FastTree⁷⁸ v2.1.11 with default parameters,
429 and examined manually with Figtree v1.4.3 (<http://tree.bio.ed.ac.uk/software/figtree/>).
430 Alignments were inspected with Aliview⁷⁹ v1.26 80, and pruned from contaminants, paralogs
431 or spurious sequences. Markers with complex histories were removed from the dataset,
432 resulting in a selection of 303 protein-coding genes. For final multi-marker phylogenetic
433 analyses and to limit computational load, the taxon sampling was reduced to 101 eukaryotes,
434 keeping at least five representatives for each known supergroup, mostly free-living
435 heterotrophic flagellates. Finally, the markers were realigned, trimmed and concatenated with

436 alvert.py from the barrel-o-monkeys
437 (<http://rogerlab.biochemistryandmolecularbiology.dal.ca/Software/Software.htm#Monkeybar>
438 rel), generating a concatenated matrix with 97,171 amino acidic sites that was used to infer
439 phylogenies (10.6084/m9.figshare.22148027). The Maximum likelihood (ML) phylogenetic
440 tree was inferred using IQ-TREE⁸⁰ v1.6 using the PMSF approximation⁸¹ and a guide tree
441 inferred with the LG+C60+F+G mixture model. Statistical support was generated with 1,000
442 ultrafast bootstraps. The Bayesian inference (BI) analyses were conducted with PhyloBayes-
443 MPI⁸² v1.5a 81 with both CAT-Poisson and CAT-GTR models⁸³, with two and four MCMC
444 chains respectively run for 10,000 generations, saving one every 10 trees. Analyses were
445 stopped once convergence thresholds were reached (i.e. maximum discrepancy <0.1 and
446 minimum effective size >100, calculated using bpcomp) and consensus trees constructed after
447 a burn-in of 25%. Additionally, to minimize possible systematic errors, the fastest-evolving
448 sites were progressively removed at 5% of sites at a time. For that, among-site substitution rates
449 were inferred using IQ-TREE under the -wsr option and the best-fitting model, generating a
450 total of 19 new data subsets (10.6084/m9.figshare.22148027). Each of them was used to infer
451 a phylogeny using IQTREE with the LG+C60+F+G model and obtain the bootstrap supports
452 for each split. We used CONSENSE from the PHYLIP v3.695 package
453 (<https://phylipweb.github.io/phylip/>) to interrogate the UFBOOT files using a Python script
454 (Nick Irwin, pers. comm.).

455

456 **Data availability**

457 Raw read sequences have been submitted to Sequence Read Archive under BioProject
458 PRJNA907040; the specific accession numbers for each protist transcriptome are given in
459 Supplementary Table 1. Transcripts and oligopeptides generated in this study are available in
460 the figshare repository (10.6084/m9.figshare.22148027).

461

462

463 **References**

- 1 Eme, L., Sharpe, S. C., Brown, M. W. & Roger, A. J. On the age of eukaryotes: evaluating evidence from fossils and molecular clocks. *Cold Spring Harb. Perspect. Biol.* **6**, a016139 (2014).
- 2 Brocks, J. J. *et al.* Lost world of complex life and the late rise of the eukaryotic crown. *Nature* **618**, 767-773 (2023).
- 3 Koonin, E. V. The incredible expanding ancestor of eukaryotes. *Cell* **140**, 606-608 (2010).
- 4 Adl, S. M. *et al.* Revisions to the Classification, Nomenclature, and Diversity of Eukaryotes. *J. Eukaryot. Microbiol.* **66**, 4-119 (2019).
- 5 Burki, F., Roger, A. J., Brown, M. W. & Simpson, A. G. B. The New Tree of Eukaryotes. *Trends Ecol. Evol.* **35**, 43-55 (2020).
- 6 Moreira, D. & López-García, P. Molecular ecology of microbial eukaryotes unveils a hidden world. *Trends Microbiol.* **10**, 31-38 (2002).
- 7 Burki, F., Sandin, M. M. & Jamy, M. Diversity and ecology of protists revealed by metabarcoding. *Curr. Biol.* **31**, R1267-r1280 (2021).
- 8 Torruella, G. *et al.* Global transcriptome analysis of the aphelid *Paraphelidium tribonemae* supports the phagotrophic origin of fungi. *Communications biology* **1**, 231 (2018).
- 9 Worden, A. Z. *et al.* Rethinking the marine carbon cycle: factoring in the multifarious lifestyles of microbes. *Science* **347**, 1257594 (2015).

482 10 AlJewari, C. & Baldauf, S. L. Conflict over the Eukaryote Root Resides in Strong Outliers,
483 Mosaics and Missing Data Sensitivity of Site-Specific (CAT) Mixture Models. *Syst. Biol.*
484 **72**, 1-16 (2023).

485 11 Roger, A. J. & Hug, L. A. The origin and diversification of eukaryotes: problems with
486 molecular phylogenetics and molecular clock estimation. *Philos. Trans. R. Soc. Lond. B
487 Biol. Sci.* **361**, 1039-1054 (2006).

488 12 Eme, L. & Tamarit, D. Microbial Diversity and Open Questions about the Deep Tree of
489 Life. *Genome Biol. Evol.* **16**, evae053 (2024).

490 13 del Campo, J. *et al.* The others: our biased perspective of eukaryotic genomes. *Trends
491 Ecol. Evol.* **29**, 252-259 (2014).

492 14 Galindo, L. J. *et al.* Phylogenomics Supports the Monophyly of Aphelids and Fungi and
493 Identifies New Molecular Synapomorphies. *Syst. Biol.* **72**, 505-515 (2023).

494 15 Ruiz-Trillo, I., Kin, K. & Casacuberta, E. The Origin of Metazoan Multicellularity: A
495 Potential Microbial Black Swan Event. *Annu. Rev. Microbiol.* **77**, 499-516 (2023).

496 16 Brown, M. W. *et al.* Phylogenomics demonstrates that breviate flagellates are related to
497 opisthokonts and apusomonads. *Proc. Biol. Sci.* **280**, 20131755 (2013).

498 17 Cavalier-Smith, T. The phagotrophic origin of eukaryotes and phylogenetic classification
499 of Protozoa. *Int. J. Syst. Evol. Microbiol.* **52**, 297-354. (2002).

500 18 Richards, T. A. & Cavalier-Smith, T. Myosin domain evolution and the primary
501 divergence of eukaryotes. *Nature* **436**, 1113-1118 (2005).

502 19 Derelle, R. *et al.* Bacterial proteins pinpoint a single eukaryotic root. *Proc. Natl. Acad. Sci.
503 U. S. A.* **112**, E693-699 (2015).

504 20 Heiss, A. A. *et al.* Combined morphological and phylogenomic re-examination of
505 malawimonads, a critical taxon for inferring the evolutionary history of eukaryotes. *Royal
506 Society open science* **5**, 171707 (2018).

507 21 Lax, G. *et al.* Hemimastigophora is a novel supra-kingdom-level lineage of eukaryotes.
508 *Nature* **564**, 410-414 (2018).

509 22 Brown, M. W. *et al.* Phylogenomics Places Orphan Protistan Lineages in a Novel
510 Eukaryotic Super-Group. *Genome Biol. Evol.* **10**, 427-433 (2018).

511 23 Atkins, M. S., McArthur, A. G. & Teske, A. P. Ancyromonadida: A new phylogenetic
512 lineage among the protozoa closely related to the common ancestor of metazoans, fungi,
513 and choanoflagellates (Opisthokonta). *J. Mol. Evol.* **51**, 278-285 (2000).

514 24 Tikhonenkov, D. V. *et al.* Microbial predators form a new supergroup of eukaryotes.
515 *Nature* **612**, 714-719 (2022).

516 25 Janouškovec, J. *et al.* A New Lineage of Eukaryotes Illuminates Early Mitochondrial
517 Genome Reduction. *Curr. Biol.* **27**, 3717-3724.e3715 (2017).

518 26 Galindo, L. J., López-García, P. & Moreira, D. First Molecular Characterization of the
519 Elusive Marine Protist *Meteora sporadica*. *Protist* **173**, 125896 (2022).

520 27 Eglit, Y. *et al.* Meteora sporadica, a protist with incredible cell architecture, is related to
521 Hemimastigophora. *Curr. Biol.* **34**, 451-459.e456 (2024).

522 28 Karpov, S. A. & Mylnikov, A. P. Biology and ultrastructure of colourless flagellates
523 Apusomonadida ord. n. *Zool Zh* **68**, 5-17 (in Russian) (1989).

524 29 Torruella, G., Moreira, D. & Lopez-Garcia, P. Phylogenetic and ecological diversity of
525 apusomonads, a lineage of deep-branching eukaryotes. *Environ. Microbiol. Rep.* **9**, 113-
526 119 (2017).

527 30 Fenchel, T. in *Adv. Microb. Ecol.* (ed K. C. Marshall) 57-97 (Springer US, 1986).

528 31 Torruella, G. *et al.* Expanding the molecular and morphological diversity of
529 Apusomonadida, a deep-branching group of gliding bacterivorous protists. *J. Eukaryot.
530 Microbiol.* **70**, e12956 (2023).

531 32 Yubuki, N. *et al.* Molecular and morphological characterization of four new ancyromonad
532 genera and proposal for an updated taxonomy of the Ancyromonadida. *J. Eukaryot. Microbiol.* **70**, e12997 (2023).

533 33 Simao, F. A., Waterhouse, R. M., Ioannidis, P., Kriventseva, E. V. & Zdobnov, E. M.
534 BUSCO: assessing genome assembly and annotation completeness with single-copy
535 orthologs. *Bioinformatics* **31**, 3210-3212 (2015).

536 34 Cavalier-Smith, T. *et al.* Multigene eukaryote phylogeny reveals the likely protozoan
537 ancestors of opisthokonts (animals, fungi, choanozoans) and Amoebozoa. *Mol. Phylogenet. Evol.* **81**, 71-85 (2014).

538 35 Derelle, R. & Lang, B. F. Rooting the eukaryotic tree with mitochondrial and bacterial
539 proteins. *Mol. Biol. Evol.* **29**, 1277-1289 (2012).

540 36 Torruella, G. *et al.* Phylogenomics reveals convergent evolution of lifestyles in close
541 relatives of animals and fungi. *Curr. Biol.* **25**, 2404-2410 (2015).

542 37 Molina, F. I. & Nerad, T. A. Ultrastructure of Amastigomonas bermudensis ATCC 50234
543 sp. nov.: A new heterotrophic marine flagellate. *European journal of protistology* **27**, 386-
544 396 (1991).

545 38 Cavalier-Smith, T. Early evolution of eukaryote feeding modes, cell structural diversity,
546 and classification of the protozoan phyla Loukozoa, Sulcozoa, and Choanozoa. *European
547 journal of protistology* **49**, 115-178 (2013).

548 39 Glücksmann, E., Snell, E. A. & Cavalier-Smith, T. Phylogeny and evolution of
549 Planomonadida (Sulcozoa): eight new species and new genera Fabomonas and
550 Nutomonas. *European journal of protistology* **49**, 179-200 (2013).

551 40 Simpson, A. G., Inagaki, Y. & Roger, A. J. Comprehensive multigene phylogenies of
552 excavate protists reveal the evolutionary positions of "primitive" eukaryotes. *Mol. Biol.
553 Evol.* **23**, 615-625 (2006).

554 41 Parfrey, L. W. *et al.* Broadly sampled multigene analyses yield a well-resolved eukaryotic
555 tree of life. *Syst. Biol.* **59**, 518-533 (2010).

556 42 Cavalier-Smith, T. Kingdom Chromista and its eight phyla: a new synthesis emphasising
557 periplastid protein targeting, cytoskeletal and periplastid evolution, and ancient
558 divergences. *Protoplasma* **255**, 297-357 (2018).

559 43 Galindo, L. J., Prokina, K., Torruella, G., López-García, P. & Moreira, D. Maturases and
560 Group II Introns in the Mitochondrial Genomes of the Deepest Jakobid Branch. *Genome
561 Biol. Evol.* **15** (2023).

562 44 Stairs, C. W. *et al.* Anaeramoebae are a divergent lineage of eukaryotes that shed light on
563 the transition from anaerobic mitochondria to hydrogenosomes. *Curr. Biol.* **31**, 5605-
564 5612.e5605 (2021).

565 45 Strassert, J. F. H., Jamy, M., Mylnikov, A. P., Tikhonenkov, D. V. & Burki, F. New
566 Phylogenomic Analysis of the Enigmatic Phylum Telonemia Further Resolves the
567 Eukaryote Tree of Life. *Mol. Biol. Evol.* **36**, 757-765 (2019).

568 46 Schön, M. E. *et al.* Single cell genomics reveals plastid-lacking Picozoa are close relatives
569 of red algae. *Nat Commun* **12**, 6651 (2021).

570 47 Heiss, A. A., Walker, G. & Simpson, A. G. The microtubular cytoskeleton of the
571 apusomonad *Thecamonas*, a sister lineage to the opisthokonts. *Protist* **164**, 598-621
572 (2013).

573 48 Jeong, D. H., Lee, H. B., Heiss, A. A., Cho, B. C. & Park, J. S. Morphological,
574 phylogenetic and biogeographic characterizations of three heterotrophic nanoflagellates
575 isolated from coastal areas of Korea. *Mar. Biol. Res.* **19**, 407-418 (2023).

576 49 Heiss, A. A., Brown, M. W. & Simpson, A. G. B. in *Handbook of the Protists* (eds John
577 M. Archibald *et al.*) 1-27 (Springer International Publishing, 2016).

578 579

580 50 Cavalier-Smith, T. & Chao, E. E. Phylogeny and evolution of apusomonadida (protozoa:
581 apusozoa): new genera and species. *Protist* **161**, 549-576 (2010).

582 51 Suzuki-Tellier, S., Kiørboe, T. & Simpson, A. G. B. The function of the feeding groove of
583 'typical excavate' flagellates. *J. Eukaryot. Microbiol.* **71**, e13016 (2024).

584 52 Heiss, A. A. *et al.* Description of *Imasa heleensis*, gen. nov., sp. nov. (Imasidae, fam. nov.),
585 a Deep-Branching Marine Malawimonad and Possible Key Taxon in Understanding Early
586 Eukaryotic Evolution. *J. Eukaryot. Microbiol.* **68**, e12837 (2021).

587 53 Cavalier-Smith, T. Ciliary transition zone evolution and the root of the eukaryote tree:
588 implications for opisthokont origin and classification of kingdoms Protozoa, Plantae, and
589 Fungi. *Protoplasma* **259**, 487-593 (2022).

590 54 Yubuki, N. & Leander, B. S. Evolution of microtubule organizing centers across the tree
591 of eukaryotes. *Plant J.* **75**, 230-244 (2013).

592 55 Carvalho-Santos, Z., Azimzadeh, J., Pereira-Leal, J. B. & Bettencourt-Dias, M. Evolution:
593 Tracing the origins of centrioles, cilia, and flagella. *J. Cell Biol.* **194**, 165-175 (2011).

594 56 Yabuki, A., Ishida, K. & Cavalier-Smith, T. *Rigifila ramosa* n. gen., n. sp., a filose
595 apusozoan with a distinctive pellicle, is related to Micronuclearia. *Protist* **164**, 75-88
596 (2013).

597 57 Glucksman, E. *et al.* The novel marine gliding zooflagellate genus Mantamonas
598 (Mantamonadida ord. n.: Apusozoa). *Protist* **162**, 207-221 (2011).

599 58 Blaz, J. *et al.* One high quality genome and two transcriptome datasets for new species of
600 Mantamonas, a deep-branching eukaryote clade. *Scientific data* **10**, 603 (2023).

601 59 Cavalier-Smith, T. & Chao, E. E. Phylogeny of choanozoa, apusozoa, and other protozoa
602 and early eukaryote megaevolution. *J. Mol. Evol.* **56**, 540-563. (2003).

603 60 Ocaña-Pallarès, E. *et al.* Divergent genomic trajectories predate the origin of animals and
604 fungi. *Nature* **609**, 747-753 (2022).

605 61 Tekle, Y. I., Wang, F., Wood, F. C., Anderson, O. R. & Smirnov, A. New insights on the
606 evolutionary relationships between the major lineages of Amoebozoa. *Sci. Rep.* **12**, 11173
607 (2022).

608 62 McCartney, B. & Dudin, O. Cellularization across eukaryotes: Conserved mechanisms and
609 novel strategies. *Curr. Opin. Cell Biol.* **80**, 102157 (2023).

610 63 Andrews, S. Vol. Available online at:
611 <http://www.bioinformatics.babraham.ac.uk/projects/fastqc/> (Cambridge, United
612 Kingdom, 2010).

613 64 Bankevich, A. *et al.* SPAdes: a new genome assembly algorithm and its applications to
614 single-cell sequencing. *J. Comput. Biol.* **19**, 455-477 (2012).

615 65 Simion, P. *et al.* A software tool 'CroCo' detects pervasive cross-species contamination in
616 next generation sequencing data. *BMC Biol.* **16**, 28 (2018).

617 66 Fu, L., Niu, B., Zhu, Z., Wu, S. & Li, W. CD-HIT: accelerated for clustering the next-
618 generation sequencing data. *Bioinformatics* **28**, 3150-3152 (2012).

619 67 Parks, D. H. *et al.* GTDB: an ongoing census of bacterial and archaeal diversity through a
620 phylogenetically consistent, rank normalized and complete genome-based taxonomy.
621 *Nucleic Acids Res.* **50**, D785-d794 (2022).

622 68 Goodacre, N., Aljanahi, A., Nandakumar, S., Mikailov, M. & Khan Arifa, S. A Reference
623 Viral Database (RVDB) To Enhance Bioinformatics Analysis of High-Throughput
624 Sequencing for Novel Virus Detection. *mSphere* **3**, 10.1128/mspheredirect.00069-00018
625 (2018).

626 69 Bigot, T., Temmam, S., Pérot, P. & Eloit, M. RVDB-prot, a reference viral protein
627 database and its HMM profiles. *F1000Research* **8**, 530 (2019).

628 70 Buchfink, B., Xie, C. & Huson, D. H. Fast and sensitive protein alignment using
629 DIAMOND. *Nature methods* **12**, 59-60 (2015).

630 71 Cantalapiedra, C. P., Hernández-Plaza, A., Letunic, I., Bork, P. & Huerta-Cepas, J.
631 eggNOG-mapper v2: Functional Annotation, Orthology Assignments, and Domain
632 Prediction at the Metagenomic Scale. *Mol. Biol. Evol.* **38**, 5825-5829 (2021).

633 72 Leger, M. M. *et al.* Organelles that illuminate the origins of Trichomonas hydrogenosomes
634 and Giardia mitosomes. *Nature ecology & evolution* **1**, 0092 (2017).

635 73 Burki, F. *et al.* Untangling the early diversification of eukaryotes: a phylogenomic study
636 of the evolutionary origins of Centrohelida, Haptophyta and Cryptista. *Proc. Biol. Sci.* **283**,
637 20152802 (2016).

638 74 Gawryluk, R. M. R. *et al.* Non-photosynthetic predators are sister to red algae. *Nature* **572**,
639 240-243 (2019).

640 75 Tikhonenkov, D. V. *et al.* New Lineage of Microbial Predators Adds Complexity to
641 Reconstructing the Evolutionary Origin of Animals. *Curr. Biol.* **30**, 4500-4509.e4505
642 (2020).

643 76 Katoh, K. & Standley, D. M. MAFFT multiple sequence alignment software version 7:
644 improvements in performance and usability. *Mol. Biol. Evol.* **30**, 772-780 (2013).

645 77 Capella-Gutierrez, S., Silla-Martinez, J. M. & Gabaldon, T. trimAl: a tool for automated
646 alignment trimming in large-scale phylogenetic analyses. *Bioinformatics* **25**, 1972-1973
647 (2009).

648 78 Price, M. N., Dehal, P. S. & Arkin, A. P. FastTree 2--approximately maximum-likelihood
649 trees for large alignments. *PLoS One* **5**, e9490 (2010).

650 79 Larsson, A. AliView: a fast and lightweight alignment viewer and editor for large datasets.
651 *Bioinformatics* **30**, 3276-3278 (2014).

652 80 Nguyen, L. T., Schmidt, H. A., von Haeseler, A. & Minh, B. Q. IQ-TREE: a fast and
653 effective stochastic algorithm for estimating maximum-likelihood phylogenies. *Mol. Biol.*
654 *Evol.* **32**, 268-274 (2015).

655 81 Wang, H. C., Minh, B. Q., Susko, E. & Roger, A. J. Modeling site heterogeneity with
656 posterior mean site frequency profiles accelerates accurate phylogenomic estimation. *Syst.*
657 *Biol.* **67**, 216–235 (2018).

658 82 Lartillot, N., Rodrigue, N., Stubbs, D. & Richer, J. PhyloBayes MPI: phylogenetic
659 reconstruction with infinite mixtures of profiles in a parallel environment. *Syst. Biol.* **62**,
660 611-615 (2013).

661 83 Rodrigue, N. & Lartillot, N. Site-heterogeneous mutation-selection models within the
662 PhyloBayes-MPI package. *Bioinformatics* **30**, 1020-1021 (2014).

663

664 Acknowledgements

665 We are grateful to Tom Cavalier-Smith and Emma Chao for their contribution to evolutionary
666 protistology and their friendly availability to discuss ideas and share protist strains. We thank
667 Ares Rocañín-Arjó, Saioa Manzano, Moisès Gil, Xavier Grau-Bové and Nick Irwin for
668 bioinformatic insights. We thank the UNICELL platform (<http://www.deemteam.fr/en/unicell>)
669 for help in transcriptome production. This work was supported by the European Research
670 Council (ERC) Advanced Grants ‘Protistworld’ and ‘Plast-Evol’ (322669 and 787904,
671 respectively) and the Horizon 2020 research and innovation programme under the Marie
672 Skłodowska-Curie ITN project SINGEK (<http://www.singek.eu/>; grant agreement no. H2020-
673 MSCA-ITN-2015-675752). G.T. was supported by 2019 BP 00208, Beatriu de Pinós-3
674 Postdoctoral Programme (BP3), Grant agreement ID: 801370. LG was funded by the Horizon
675 2020 research and innovation programme under the European Marie Skłodowska-Curie
676 Individual Fellowship H2020-MSCA-IF-2020 (grant agreement no. 101022101-FungEye).

677

678 **Figure legends**

679

680 **Figure 1. Phylogenomic tree of eukaryotes including an expanded diversity of**
681 **Apusomonadida and Ancyromonadida.** The tree was inferred using Maximum Likelihood
682 from 97,171 amino acid positions and 101 taxa (model of sequence evolution: LG+C60+F+G
683 – PMSF). The root of the tree has been arbitrarily placed between Metamonada and the rest of
684 eukaryotes. Numbers at nodes represent ultrafast bootstrap approximation percentages (1,000
685 replicates) followed by Bayesian posterior probabilities under CAT-GTR and CAT-Poisson
686 models, respectively. Black dots denote maximum support with all methods. The scale bar
687 indicates the number of expected substitutions per unit branch length. The asterisks indicate
688 taxa of typical excavates.

689

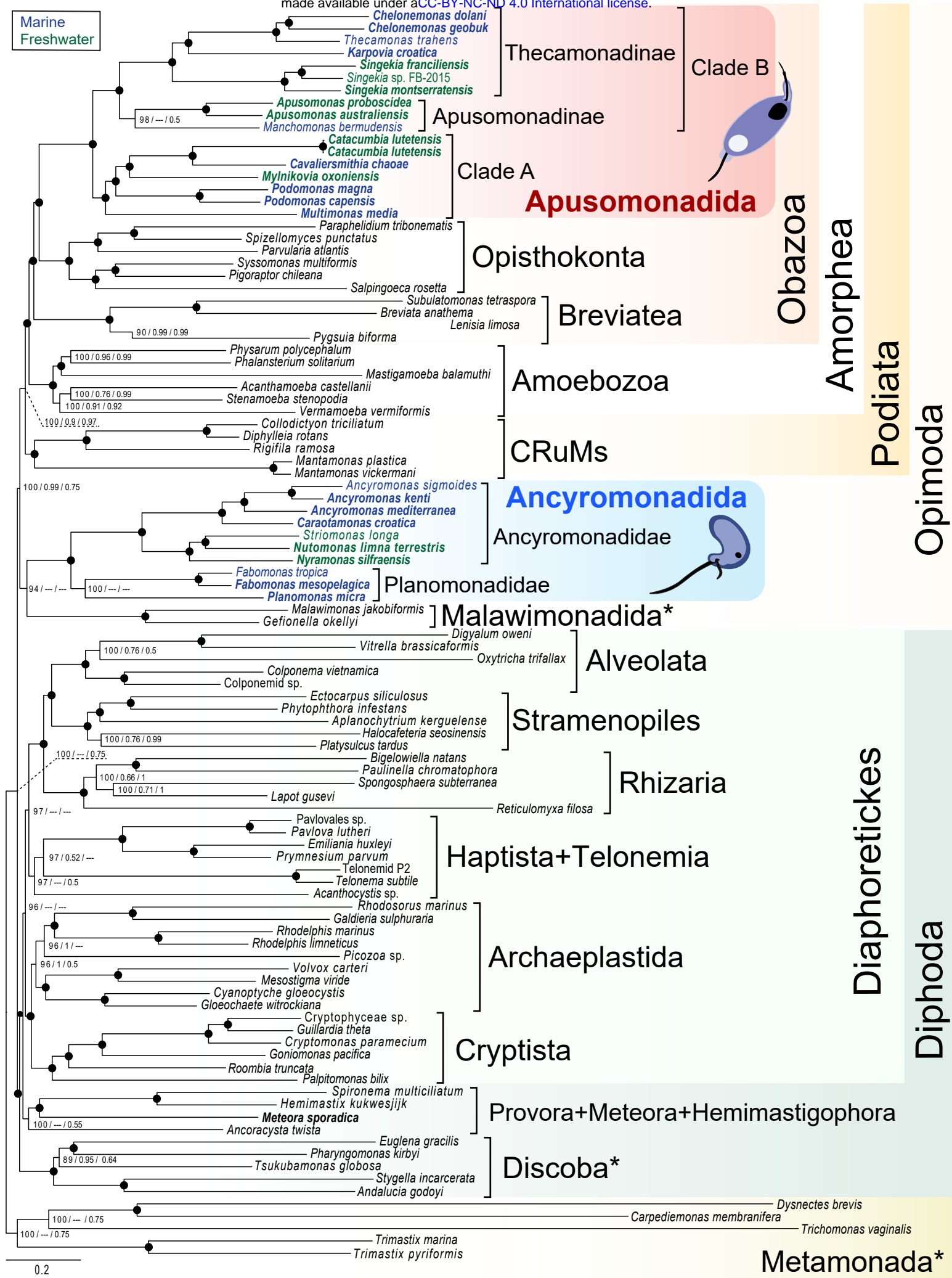
690 **Figure 2. Progressive removal of the fastest evolving sites in 5% increments to evaluate**
691 **alternative topologies within Opimoda.** The alternative positions tested were as follows. **a**,
692 Within the Apusomonadida: *Manchomonas* being sister to *Apusomonas* or to the
693 Thecamonadinae (dashed line). **b**, Within the Ancyromonadida: the monophyly of *Fabomonas*
694 and *Planomonas* (the Planomonadidae clade) versus their paraphyly (*Fabomonas* branching
695 deeply, dashed line). **c**, Regarding the placement of Malawimonadida and Ancyromonadida:
696 Malawimonadida and Ancyromonadida being monophyletic versus Malawimonadida
697 branching as sister to Podiata (and, accordingly, ancyromonads as the earliest-branching
698 Opimoda lineage) or Malawimonadida sister to Discoba (dashed lines). **d**, Plot showing the
699 bootstrap support in ML phylogenetic trees under the LG+C60+F+G model of sequence
700 evolution as sites are progressively removed. The monophyly of Opisthokonta (yellow) is used
701 as a control to indicate when the phylogenetic signal is too low to retrieve well-known robust
702 monophyletic clades.

703

704 **Figure 3. Early trait evolution across Opimoda lineages.** The distribution of five key
705 morphological traits is parsimoniously inferred for each lineage ancestor (upper panel) based
706 on available descriptions and, to their respective last common ancestors (LCA), based on the
707 inferred phylogenetic backbone (lower panel). Numbers in black circles refer to the number of
708 flagella. The small character drawings in the cladogram represent the innovations at the onset
709 of each lineage.

710

711



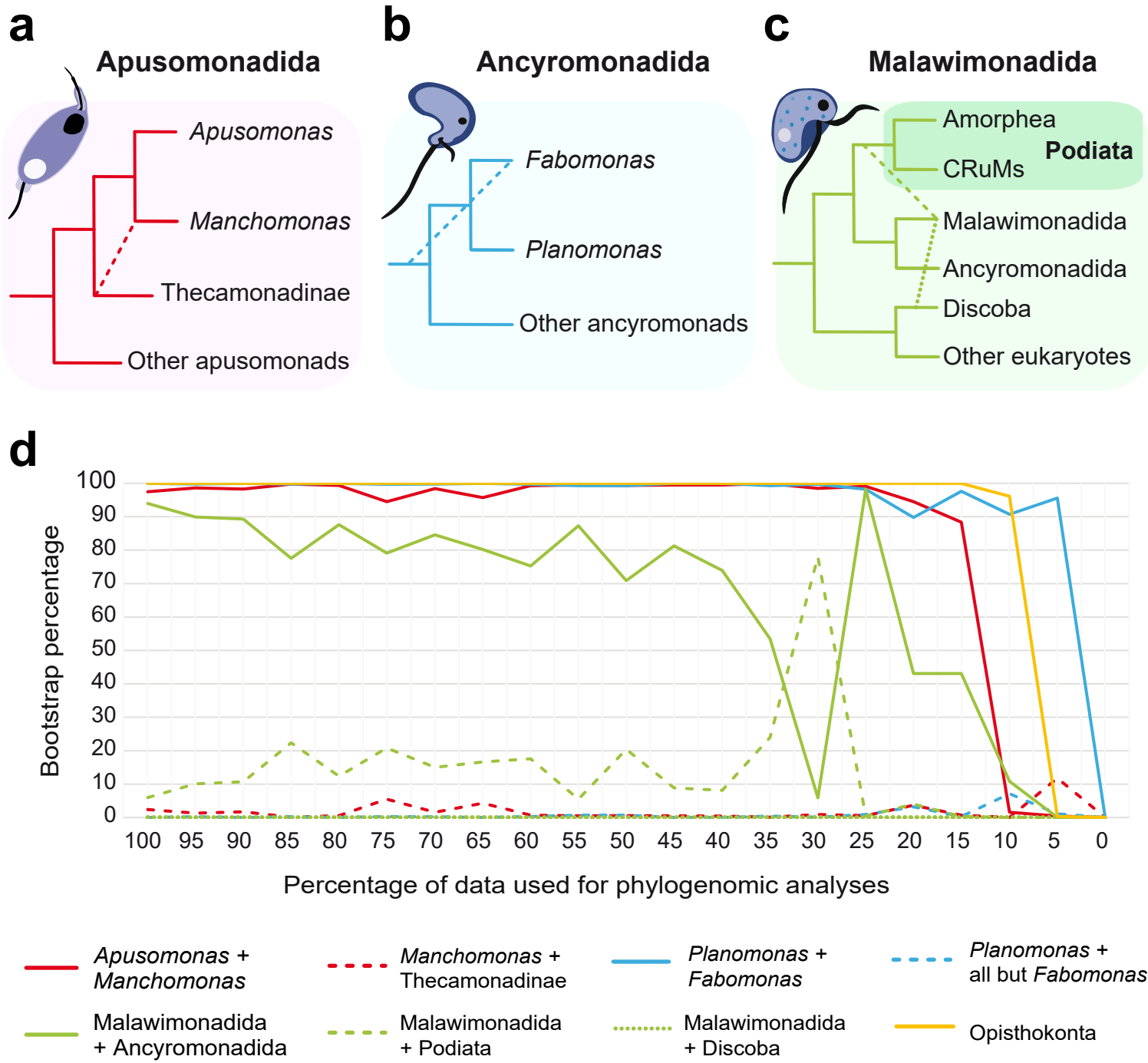


Figure 2

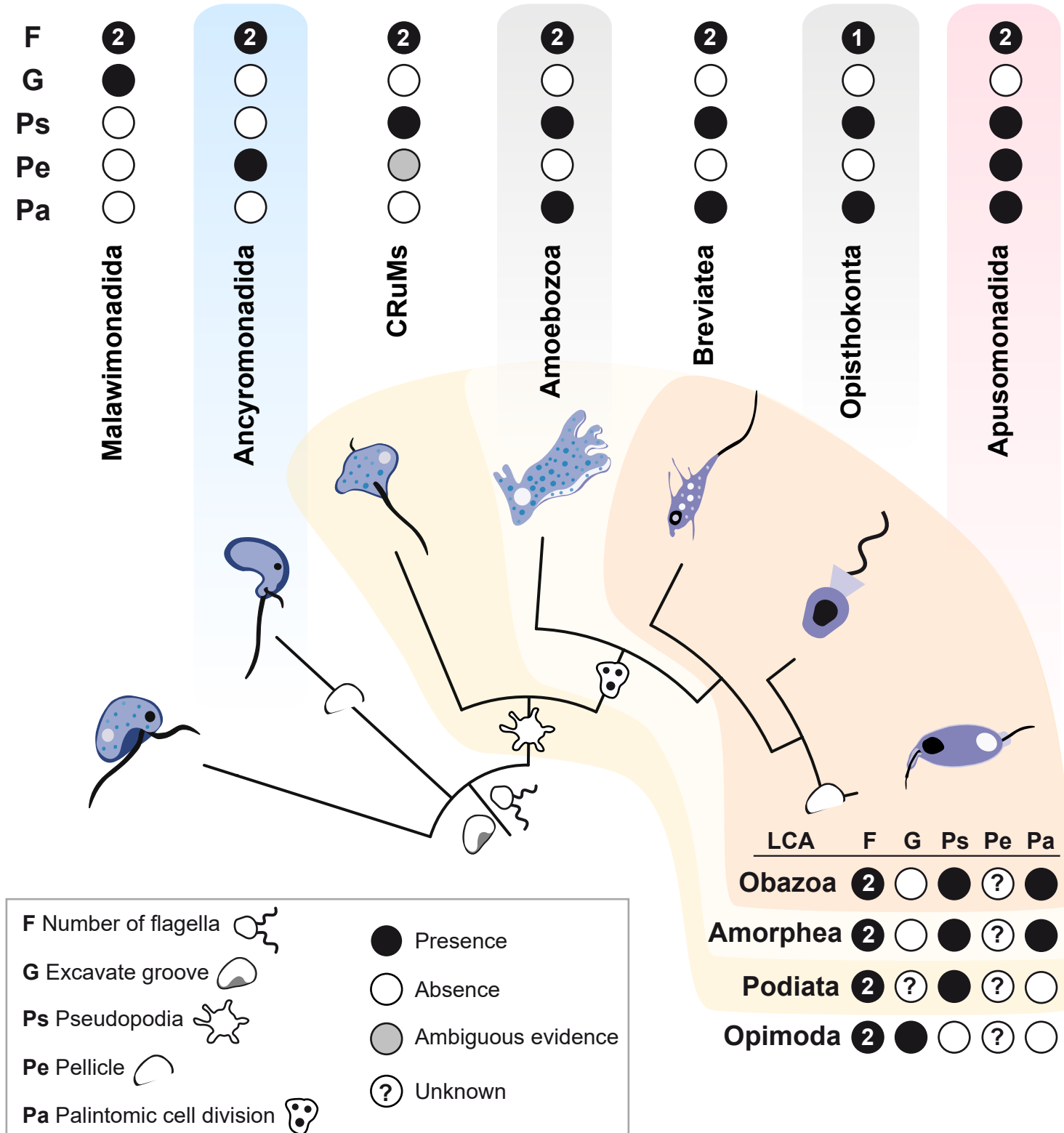


Figure 3